Review TRENDS in Neurosciences Vol.28 No.11 November 2005

The anatomical logic of smell

Thomas A. Schoenfeld[1] and Thomas A. Cleland[2]

[1]Department of Physiology and Program in Neuroscience, University of Massachusetts Medical School, Worcester, MA 01655, USA
[2]Department of Neurobiology and Behavior, Cornell University, Ithaca, NY 14853, USA

Olfactory receptor neurons (ORNs) expressing the same odorant receptor gene share ligand–receptor affinity profiles and converge onto common glomerular targets in the brain. The activation patterns of different ORN populations, evoked by differential binding of odorant molecular moieties, constitute the primary odor representation. However, odorants possess properties other than receptor-binding sites that can contribute to odorant discrimination. Among terrestrial vertebrates, odorant sorptiveness – volatility and water solubility – imposes physicochemical constraints on migration through the nose during inspiration. The non-uniform distributions of ORN populations along the inspiratory axis enable sorptiveness to modify odor representations by affecting the number of molecules reaching different receptors during a sniff. Animals can then modify and analyze odor representation further by the dynamic regulation of sniffing.

Introduction

Discovery of the odorant receptor (OR) gene repertoire [1] has fostered many subsequent findings that together help to define how olfactory receptor neurons (ORNs) and their membrane ORs recognize and distinguish odorant molecules – what has been called the 'molecular logic' of the sense of smell [2]. Prominent among these findings is the observation that ORNs expressing the same OR gene display precise convergence of axonal projections onto the same target sites in the brain, known as glomeruli [3–6] (Figure 1). In vertebrates, glomeruli are discrete neuropilar zones of synaptic interaction between ORNs and olfactory bulb neurons that appear to be unit modules for the representation and processing of sensory features, displaying molecular receptive fields comparable to those of their constituent ORNs [7,8]. This pattern of glomerular convergence, along with the segregation of different OR gene populations via ORN axonal projections onto mutually exclusive glomeruli, generates a chemospecific (odotopic) map in the brain that reflects the selective binding of particular molecular moieties (odotopes) to particular ORs [8–12]. This odotopic map sets the stage for combinatorial, parallel processing of information about distinct molecular moieties, contributing to odorant identification [13–15].

There is significant intermingling of different ORN populations within the olfactory epithelium (OE) that lines the nasal cavity. Because it has been generally assumed that the distribution of sampled molecules along the OE is effectively random, most presume that olfactory stimuli are represented solely by their profiles of odotope–receptor affinities, without the distinct spatial component found in other sensory modalities [16–18]. Indeed, it is unlikely that there is any explicit representation of the location of odorants in external space by the olfactory system. Olfactory-guided spatial tasks, such as tracking in rats, rely on a more complex, iterative program of behavioral integration based on repeated sampling from different locations [19]. However, in addition to the odotopic maps in their brains, several species exhibit suggestive spatial patterns in OR gene expression across the nasal epithelium [20,21] that could contribute to odotopic processing. Rodents in particular, and perhaps other long-snouted terrestrial vertebrates, appear to have specific anatomical adaptations enabling the use of intranasal space as an additional stimulus-differentiating factor for odorant molecules. In this review, we discuss the evidence for and potential utility of these putative adaptations,

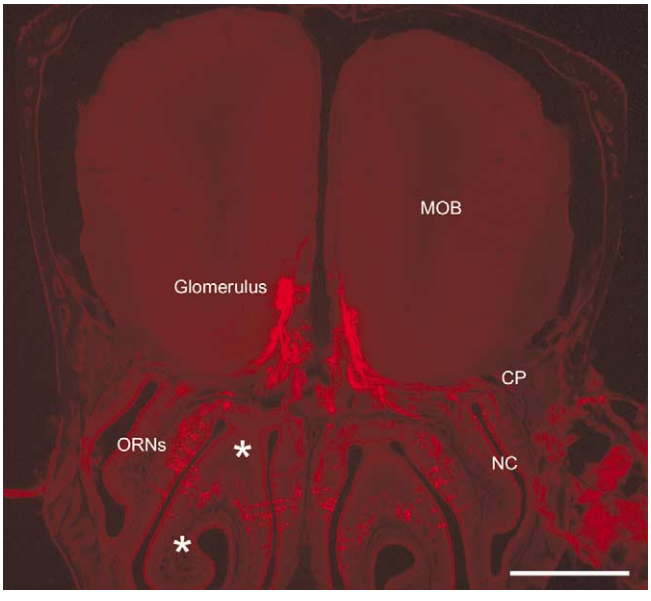

Figure 1. Convergence of olfactory receptor neurons (ORNs) onto glomeruli in the main olfactory bulb (MOB). Homologous populations of odorant receptor (OR)-gene-specific ORNs lining each nasal cavity (NC) project their axons onto homologous glomeruli in the MOB. Here, mouse ORNs expressing the P2 receptor gene and lining the medial recesses of each nasal cavity converge onto medially positioned glomeruli in each MOB. These ORNs exhibit a restricted, zonal distribution within the nasal cavity, confined within a narrow band extending in a semicircle across the cavity on each side (asterisks indicate zones above and below this band). This coronal section was taken from a P2-IRES-tau-*lacZ* mouse, in which ORNs that express the P2 gene also synthesized β-galactosidase [6], which is visualized here using immunofluorescence (processing and photograph courtesy of J. Crandall). Additional abbreviation: CP, cribriform plate. Scale bar, 750 μm.

Corresponding author: Schoenfeld, T.A. (thomas.schoenfeld@umassmed.edu).
Available online 21 September 2005

 0166-2236/$ - see front matter doi:10.1016/j.tins.2005.09.005

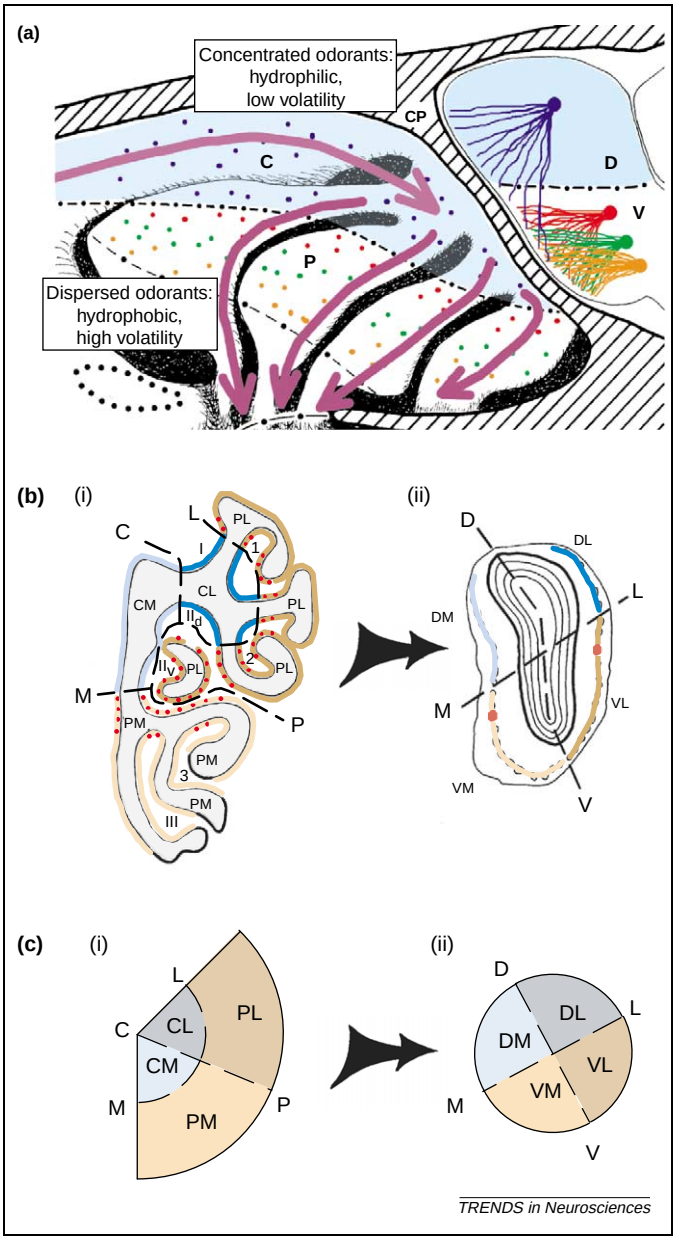

Figure 2. Organization of olfactory airspace in the rodent nose, and its relationships to inspiratory airflow and ORN projections to the MOB. **(a)** Sagittal cut-away view of the hamster nose and cranium, depicting the medial surfaces of nasal turbinates lined with olfactory epithelium (OE, left) and the medial MOB (right), separated by the cribriform plate (CP). Blue shading designates the central air domain (C), situated dorsally in the nose, and the corresponding dorsal half of the MOB in the brain (D), to which central-domain ORNs (blue dots) project. Peripheral-domain (P) ORNs (red, green and orange dots) project to the ventral MOB (V). Arrows represent inspiratory airflow paths, coursing first caudally through the central domain (from the external naris to the left) and then rostrally through the peripheral domain, before exiting at the septal window into the nasopharynx [22,23]. Inset boxes summarize the proposed relationships between the chemical properties underlying odorant sorptiveness and the spatial extent of migration along the inspiratory path through the central and peripheral domains. Movement through separate medial and lateral channels is not illustrated here. Converging lines and filled circles in the MOB represent axons from separate ORN populations, arrayed along the central–peripheral axis, that converge onto target glomeruli arrayed at corresponding positions across the dorsal–ventral axis of the MOB. Red dots, lines and circles correspond to the P2 ORN population and its projections depicted in Figure 1. (b,c) Rhinotopic regions within the nose and MOB. **(b)** Depictions of coronal sections through the nose (i) and MOB (ii). Blue outline shading denotes central-domain OE and its target glomeruli in the dorsal MOB, as in (a). Tan shading denotes peripheral-domain OE and its target glomeruli in the ventral MOB. Medial (M) and lateral (L) components of these projections are distinguished by lighter and darker shading, respectively. Red dots in (i) represent ORNs expressing the P2 odorant receptor (Figure 1), distributed just peripheral to the central–peripheral boundary, with separate medial (PM) and lateral (PL) subpopulations forming mutually exclusive projections to homologous glomeruli in the ventral-medial (VM) and ventral-lateral (VL) MOB [red dots in (ii)] [6,44,50]. Thick black lines bordering gray airspace in (i) denote nonsensory epithelium. Note that homologous medial and lateral glomeruli are not typically found in the same coronal plane, as illustrated, but rather are oriented with the lateral glomerulus positioned more rostrally. **(c)** Corresponding schematic diagrams of the central–peripheral and medial–lateral axes in the nose (i) as mapped onto the dorsal–ventral and medial–lateral axes in the MOB, respectively (ii). The diagrams idealize the nasal coordinate system as a set of concentric semi-annuli and the bulbar coordinate system as a set of obliquely oriented circular sectors. Color shading is the same as in (b). For simplicity, neither (b) nor (c) displays the longitudinal dimension depicted in (a). Additional abbreviations: CL, central-lateral; CM, central-medial; DL, dorsal-lateral; DM, dorsal-medial. I, IId, IIv, III and IV are endoturbinate extensions of the ethmoid bone; 1, 2 and 3 are ectoturbinate extensions. Modified, with permission, from [40].

which could contribute a supplementary 'anatomical logic' to the sense of smell.

Rodent intranasal anatomy comprises distinct airflow channels that induce differential odorant sorption and migration

In the rodent nose, olfactory airspace comprises anatomically distinct air channels within the olfactory recesses, which are formed by branched extensions of the ethmoid bone (turbinates). It is through these channels that air flows and odorant molecules migrate during inspiration (Figure 2). Fluid dynamic models demonstrate that, during the inspiratory phase of a sniff cycle in rodents, air entering the olfactory recesses flows first through centrally positioned domains associated with the dorsal meatus, then courses more peripherally (ventrally and laterally) through the distinct medial and lateral recesses, before exiting at the internal naris (nasopharyngeal outlet) [22,23] (Figure 2a, arrows). Fluid dynamic modeling also indicates that air flows through the medial recess at comparably high rates both centrally and peripherally (Figure 2b, CM and PM), whereas air flowing through the lateral recess slows considerably as it courses peripherally [22] (Figure 2b, CL and PL).

In following structured paths, inspiratory airflow in rodents is directed through narrow passageways that sustain laminar flow and prevent turbulence [22,23]. By contrast, airflow within the larger, less structured passageways of primate noses appears to be turbulent [24]. Turbulence reflects the disorderly lateral movement of transported molecules such as odorants out of the carrier (air) stream towards passageway walls, and it entails substantial fluctuations in flow velocity [25,26]. However, under laminar flow conditions, lateral movement is governed solely by diffusion and hence depends more on local concentration within the air stream than is the case under turbulent conditions [25]. Consequently, laminar flow is likely to better preserve minute concentration differences in the air stream that develop as odorants pass through the nose.

These concentration differences are probably odorant-specific, generated by variation in odorant sorptiveness, which encompasses several whole-molecule physicochemical properties such as volatility, hydrophobicity and water solubility [27]. Evidence from amphibians, rodents and humans [27–30] shows that the terrestrial vertebrate nose, which is lined with aqueous mucus, acts as a gas

chromatograph: it selectively adsorbs inhaled vapors from the carrier air stream such that odorant molecules migrate through the nose differentially according to their relative sorptiveness. Highly sorptive molecules such as methyl benzoate, which are hydrophilic and have low volatility, are retained by the terrestrial vertebrate nose to a greater extent than are nonsorptive odorant molecules such as nonane, which are hydrophobic and highly volatile (Figure 3). Moreover, a high degree of odorant retention is associated with an uneven distribution along the inspiratory path, with greater concentrations adsorbing to the mucus that lines earlier portions of the passageway, whereas low retention is associated with a more even distribution across the OE [27]. Laminar flow in rodent noses could accentuate this chromatographic separation during odorant migration, just as laminar flow in capillary-tube column chromatography yields separations that are superior to those achievable using packed columns that produce turbulence [31]. Furthermore, variations in inhalation dynamics (flow rate, duration and cycling) can enhance or reduce this migratory differentiation [29,30,32,33]; as in a gas chromatograph, higher flow rates will reduce sorption and enhance migration (Figure 3). Different flow rates can arise owing to the different structures of the medial and lateral recesses in rodents [22] or differences in patency between the two cavities [34], and can also be brought about behaviorally during active sniffing [34–36].

If the internal structure of the rodent nose enhances the differential migration of odorants through the olfactory recesses according to their sorptiveness, how might the rodent olfactory system make use of this differentiation?

Topographic projections map intranasal airspace onto the rodent olfactory bulb

Olfactory airspace in the rodent nose is topographically represented in the glomerular layer of the main olfactory bulb (MOB) as a rhinotopic map. This map organizes mutually exclusive projections of ORNs from longitudinally oriented nasal air channels onto longitudinally oriented sectors of the MOB, grouping ORNs and their target glomeruli by virtue of the common intranasal airspace they sample [37–40] (Figure 2). Thus, it maps broad neighborhood relationships, rather than nearest-neighbor relationships akin to the point-to-point mappings common in other sensory systems [16,41]. Specifically, the rhinotopic map segregates the parallel medial and lateral channels of inspiratory airflow in each nasal cavity, in addition to the central and peripheral domains along each path that correspond to the direction of inspiratory flow between the external and internal nares (Figure 2a). ORNs in the OE lining each channel and domain project to the MOB in a mutually exclusive pattern: the medial OE to the medial hemisphere of each MOB, the lateral OE to the lateral hemisphere, the central OE to the dorsal MOB, and the peripheral OE to the ventral MOB (Figure 2b).

The chemospecific odotopic map is composed of different populations of OR-gene-specific ORNs intermingled in

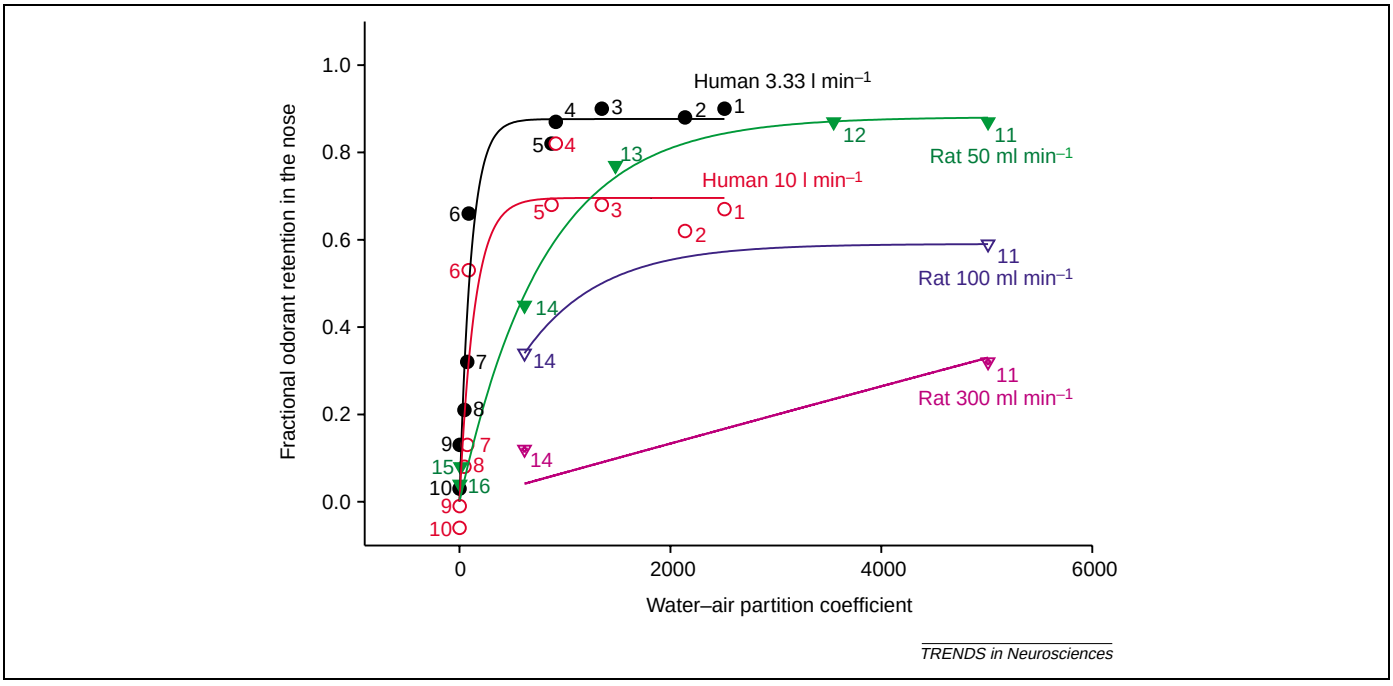

Figure 3. Relationship between odorant retention and odorant sorptiveness in the human and rat noses with respect to airflow rate. The ordinate depicts the proportion of odorant delivered into the nose that is not present in the air stream that subsequently exits the nose. Maximum retention found in these studies was ~90%. The abscissa depicts the water–air partition coefficient for each odorant, used as an index of sorptiveness (higher values denote greater sorptiveness). Coefficient values are based on Henry's Law constants as estimated using HENRYWIN™ version 3.10 (US Environmental Protection Agency, http://www.epa.gov/opptintr/exposure/docs/episuite.htm), using the group method at 25°C. High values represent high water solubility and/or polarity, and/or low volatility. Estimated coefficients are highly reliable as relative values, but can be 2–3 times higher than absolute values derived empirically [28]. Human data are based on [30]; rat data are based on [28,29]. All odorants in the human dataset were tested at both airflow rates, whereas only odorants 11 and 14 in the rat dataset were tested at the higher airflow rates. Exponential functions were fitted to the data by SigmaPlot™, using the exponential rise to maximum category and assuming origin at (0,0). All goodness-of-fit values were $R^2 > 0.90$ except for rat 300 ml min^{-1}, for which $R^2 = 0.69$. Odorants are: 1, butanol; 2, isopropyl alcohol; 3, methyl benzoate; 4, L-carvone; 5, benzaldehyde; 6, diphenyl oxide; 7, heptaldehyde; 8, amyl acetate; 9, D-limonene; 10, nonane; 11, ethanol; 12, 1-propanol; 13, isoamyl alcohol; 14, acetone; 15, bromobenzene; 16, ortho-xylene.

broad zones or focally restricted patches that are spatially aligned with the rhinotopic coordinate system and conform to its rules (Figure 2). Zonally distributed populations (e.g. M71, P2 and I7), which were once thought to be grouped into four canonical zones, are arrayed at distinct but overlapping zonal positions in a continuous distribution along the central–peripheral axis of the OE [42,43], with the bulbar projections of central domain populations directed dorsally in the MOB and those of peripheral domain populations directed ventrally [43]. Moreover, distinct medial and lateral ORN subpopulations expressing each OR gene type converge separately onto medial and lateral glomeruli, respectively [37,44].

Some ORN populations do not follow this zonal pattern. These zone-independent populations (e.g. OR37 and OR-Z6) are restricted to patches of OE close to the medial–lateral and central–peripheral boundaries in the olfactory recesses, and lack the distinguishable medial–lateral subpopulations seen in zonally distributed populations. They usually converge onto a single, unpaired glomerulus positioned rostrally near the intersection of the ventral meridian (i.e. medial–lateral boundary) and the medial and lateral meridians (i.e. dorsal–ventral boundaries) [45,46].

The potential importance of these maps to olfaction is underscored by the mechanisms employed to establish and maintain them. The basic medial–lateral and dorsal–ventral axes of the rhinotopic coordinate system appear to depend on separate systems of extracellular matrix molecules. Interactions between semaphorin 3A and neuropilin underlie the dispersion of homologous ORN populations to the medial and lateral hemispheres of the MOB [47,48]. However, OCAM/mamFasII – a member of the immunoglobulin superfamily – is associated only with the peripheral–ventral stream of projections [49,50], and so could guide differentiation of the dorsal–ventral dimension in the bulb. Finally, convergence of OR-gene-specific ORNs to specific glomeruli appears to depend on expression of the OR in the convergent axon terminals [3,11], and coexpression of different ephrins could regulate the rostral–caudal positioning of such convergence within the broader circumferential (dorsal–ventral, medial–lateral) domains of the MOB [16].

Central bulbar circuits reflect the rhinotopic map

In the MOB, numerous local circuits contribute to the processing of odotopic features [51–53]. However, there are also two extrinsic corticocortical circuits in rodent olfactory bulbs that provide a basis for integrating information derived from the parallel air channels within the nose [37,40]. Specifically, mutually inhibitory intrabulbar circuitry connects homologous medial and lateral clusters of tufted cells in each bulb that receive input from ORN subpopulations expressing the same OR but lining different channels (medial and lateral, respectively) within the nasal cavity [10,54,55]. Comparably, an interbulbar commissural circuit, involving the pars externa of the anterior olfactory nucleus, appears to be structured for association of sensory information gathered from homologous air channels in the two bilaterally symmetric nasal cavities [56]. Notably, these circuits facilitate comparison across the medial–lateral and left–right divisions of the nose (i.e. those associated with the parallel flow of odorant molecules along inspiratory paths) and exclude the central–peripheral dimension associated with serial flow. Their actual functions, however, remain largely unexplored.

Rhinotopic and odotopic mapping along the central–peripheral axis is disproportionate

Evidence is emerging that the rhinotopic and odotopic projection maps from the OE to the MOB are disproportionate along the inspiratory path (the central–peripheral rhinotopic axis). Specifically, these maps vary significantly along this axis in the convergence ratios of ORNs onto MOB glomeruli and secondary neurons. The ventral half of the MOB, which contains about half of the total number of glomeruli and secondary neurons (principally mitral and tufted cells), is innervated disproportionately by 75% of the mature ORNs across a concomitant 75% of the sensory sheet, receiving a threefold greater number of afferents than the dorsal MOB [39,40] (Figure 4). OR gene expression also is not uniform across this same axis. Central-domain (zone 1) ORNs express nearly half of all OR genes, despite representing only 25% of all ORNs and being confined to only 25% of the receptor sheet [57]. Thus, a patch of OE lining the central domain is likely to contain a greater diversity of OR-gene-specific populations than a comparably-sized patch lining the peripheral domain, but will display fewer ORNs per OR gene type (Figure 4).

This disproportionate representation along the central–peripheral dimension, which corresponds to variation in odorant sorptiveness, resembles examples of magnified representation in other sensory systems (e.g. the retinal fovea, fingers and lips in primates, whiskers in rodents, and echolocating frequencies in bats). Notably, the higher convergence ratios are found among ORNs innervating peripheral domains, where adsorbed odorant concentrations are likely to be lower. It has been proposed in theoretical and experimental studies (reviewed in [58]) that higher ORN convergence ratios lead to improved signal-to-noise ratios and greater effective sensitivity, thereby facilitating the detection and processing of what are probably weaker stimuli. By contrast, the disproportionately greater number of OR gene classes found in central-domain OE could enhance the capacity for odotopic discrimination among highly sorptive odorants in this early portion of the inspiratory path [40].

Rhinotopic contributions to odorant representations in the brain

As we have reviewed so far, inhaled odorant molecules are differentially sorbed by the terrestrial vertebrate nose, and so are likely to display distinctive migratory patterns as they move across the OE. This rhinotopic differentiation reflects whole-molecule properties, collectively known as sorptiveness, which, by affecting the delivery of odorant molecules to ORN membrane receptors, could influence odotope–receptor binding patterns in a manner independent of their binding affinities. That is, the sorptiveness of a molecule would affect the odor representation by influencing the relative activation levels of ORNs based on their physical location within the nose. However,

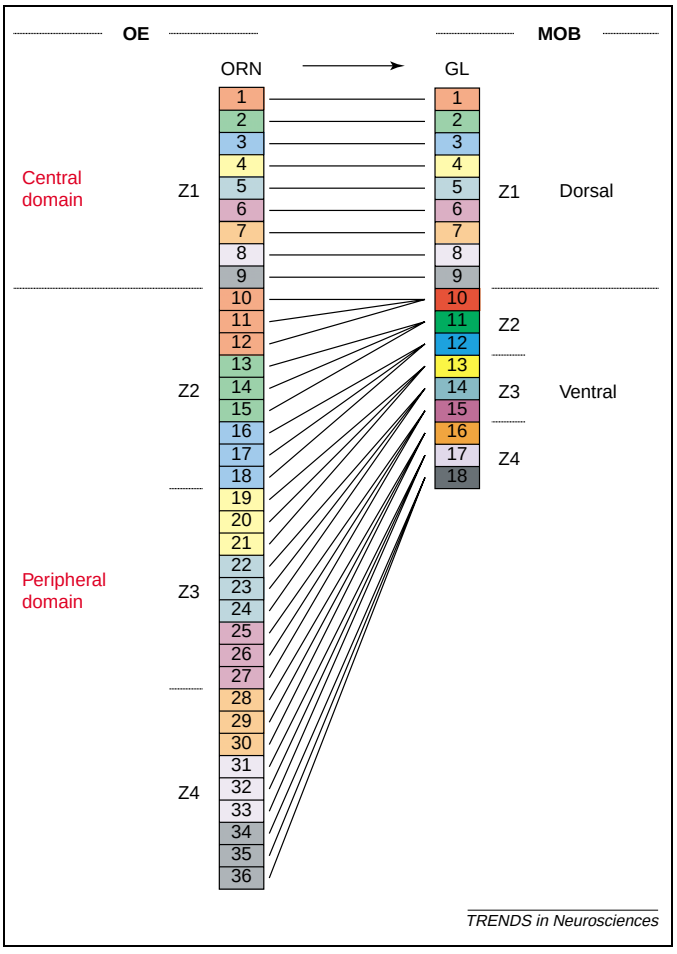

Figure 4. ORN populations vary disproportionately along the central–peripheral axis of rhinotopy. The peripheral-domain OE covers a threefold greater surface area than the central domain, with threefold more ORNs packed together at a constant density. However, in the MOB, which receives axonal projections from the ORNs, the ventral half contains the same number of glomeruli (GL) as the dorsal half. Consequently, the convergence ratio of ORNs to glomeruli is threefold higher in the peripheral-to-ventral projection (represented by more saturated color in the ventral MOB boxes) than in the central-to-dorsal projection (estimates in hamster are ~4500:1 versus ~1500:1, respectively [40]). Despite this difference in ORN numbers, the central and peripheral domains exhibit comparable diversity of odorant receptor (OR) gene classes [57], here represented by the same range of nine colors filling the ORN boxes. The ORNs associated with each OR gene class, with the exception of the few zone-independent classes [21], are distributed within restricted zones across the central–peripheral dimension, generally confined to ≤25% of the OE rather than distributed across the entire OE. The illustration shows four discrete zones (Z1–Z4) for clarity, although there is growing evidence that zonally distributed populations do not respect discrete boundaries, at least within the peripheral domain [42,43]. We assume that convergence is homotypic – that is, each glomerulus is innervated by only one class of ORN [40]. Under these constraints, the peripheral zones (Z2–Z4) will contain, on average, one-third as many ORN classes as the central zone (Z1; depicted as three colors per peripheral zone compared with nine in Z1), to accommodate threefold more ORNs per class. We propose that this translates into trade-offs between resolving power and sensitivity across the central–peripheral dimension (i.e. along the inspiratory airflow path).

for whole-molecule rhinotopic differentiation to influence representations at the glomerular level, ORs must be differentially distributed across intranasal space, because if OR distributions were homogeneous across the OE, rhinotopic differentiation would presumably be eliminated by the convergence of similarly tuned ORNs.

The zonal pattern of OR expression in rodent noses [43], aligned with intranasal airflow channels and to some extent expressing mutually exclusive receptor complements, appears to provide the necessary anisotropy. First, there is evidence in rodents that the intrinsic spatial arrangement of ORN gene classes along the inspiratory axis locates receptors for hydrophilic odotopes disproportionately in regions where greater adsorption of hydrophilic odorants is expected, akin to the cochlear tonotopic alignment of hair-cell tuning with basilar membrane mechanics [59]. Indeed, the OR genes expressed in the central domain (OR zone 1) include all of the phylogenetically old class I genes that are found in fish and amphibians, which are expected to encode ORs that are particularly sensitive to hydrophilic (i.e. sorptive) odorants [57,60]. Second, physiological recordings demonstrate that ORNs associated with the central domains are generally more responsive to highly sorptive odorants such as the carvones or benzaldehyde, whereas peripheral-domain ORNs are generally more responsive to less sorptive odorants such as limonene or octanal [9,11,14,61–63] (Figure 5). Neuronal and glomerular activity in the MOB also appears to reflect these rhinotopic contributions to odorant representations: highly sorptive molecules activate primarily dorsal glomeruli, whereas relatively nonsorptive molecules tend to have correspondingly more ventral representations [8,12] (Figure 6). Finally, recent behavioral observations also reflect this pattern. Specific lesions of central-domain OE in mice significantly raised detection thresholds for two relatively sorptive odorants (n-decyl alcohol and pyridazine) but did not alter the thresholds for two relatively nonsorptive odorants (ethyl acetate and benzene) [64].

If odorant sorptiveness and the nonuniform distribution of ORs indeed contribute to odorant representations, how might these rhinotopic influences be integrated with odotopic maps, and hence reflected in patterns of odor-evoked ORN activation? The diversity of molecules detected by ORs [7] renders it likely that ORNs in different zones will show some responsiveness to a particular odotope, and that a given odotope can be associated in principle with molecules exhibiting substantially different sorptive properties. Hence, the relative levels of binding of an odotope to each of its sensitive OR classes could be quantitatively influenced by the aggregate properties of the other odotopes of the same odorant molecule, and by the whole-molecule properties that they together determine. For example, an aldehyde end group attached to an aliphatic chain could evoke different relative levels of activation among its complement of sensitive ORNs, depending on the properties of the remainder of the molecule and the physical distribution of these sensitive ORNs along the central–peripheral axis. This additional dependency theoretically increases the available coding space for odors beyond that generated by the receptor complement alone, improving the capacity of the animal to discriminate certain odorants but still enabling recognition of similarities between odotopes on molecules of different sorptive properties.

Rhinotopy could facilitate behavioral regulation of odor sampling

Animals can dynamically modify their odorant sampling, or sniffing, by actively altering inspiratory and expiratory airflow via changes in flow rate, duration and

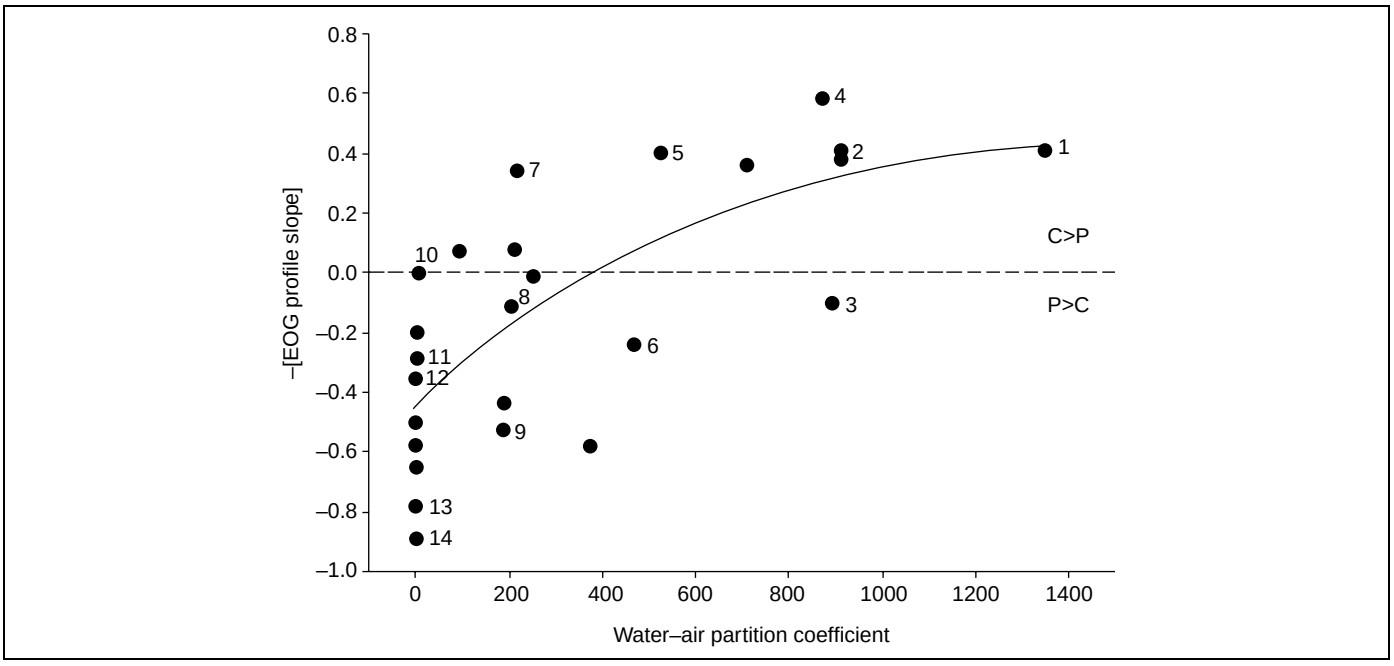

Figure 5. Relationship between odorant-evoked activity in the rat OE and odorant sorptiveness. The ordinate comprises an index of peak electro-olfactogram (EOG) amplitude recorded relative to the zonal position of the recording electrode along the central–peripheral axis, extracted as the negative value of the linear slope of the amplitude–distance function (using data from [61]; figure modified, with permission, from [65]). Positive values represent EOG amplitudes that were larger in central-domain OE than peripheral-domain OE (C > P), whereas negative values represent the inverse relationship (P > C). Amplitudes were normalized to responses to amyl acetate [61]. The abscissa depicts the water–air partition coefficient for each odorant (Figure 3). The fitted function is an exponential rise to maximum with a non-zero *y*-intercept. Goodness-of-fit was determined by SigmaPlot™: $R^2 = 0.54$. Selected odorants identified (of 25 plotted) are: 1, methyl benzoate; 2, D- and L-carvone; 3, heptanal; 4, benzaldehyde; 5, 4-ethyl benzaldehyde; 6, camphor; 7, menthone; 8, cyclohexyl acetate; 9, 1,8-cineole; 10, anisole; 11, benzene; 12, D-limonene; 13, hexane; 14, heptane.

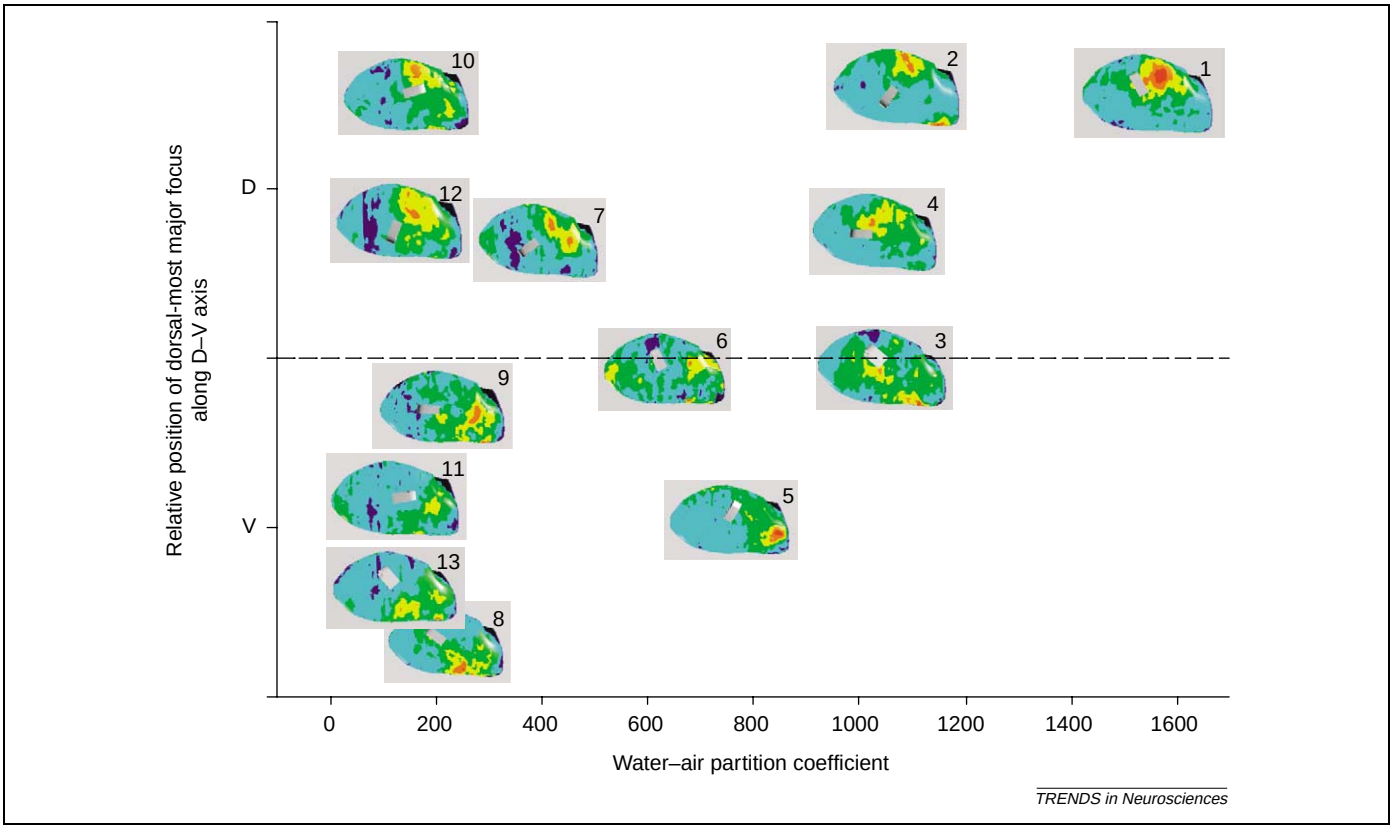

Figure 6. Relationship between the distribution of odorant-induced activity in the rat MOB and odorant sorptiveness. Images of 2-deoxyglucose activity maps for 13 odorants, produced by Johnson, Leon and colleagues (e.g. [12]), were downloaded from the Glomerular Activity Response Archive (http://leonlab.bio.uci.edu/index.html) as 3D images (medial surface, dorsal up, rostral left). Images are arrayed according to odorant sorptiveness (abscissa, denoted by the water–air partition coefficient as used in Figure 3) and the relative dorsal–ventral (D–V) position of dorsal-most major foci of activation (ordinate). Odorants are: 1, methyl benzoate; 2, L-carvone; 3, heptanol; 4, benzaldehyde; 5, acetone; 6, camphor; 7, L-menthone; 8, heptanal; 9, isoamyl acetate; 10, ethylbenzene; 11, D-limonene; 12, heptane; 13, nonane.

cycling [32,35,36,63]. As already noted, such changes influence odorant sorption and migration along the nasal passages and have consequences for odorant representations, as assessed both physiologically [33,63,65] and behaviorally [34–36]. We propose that animals with zonally organized ORN populations, such as rodents and salamanders, could specifically utilize this capacity, here called 'zonation', to direct migration of odorant molecules to different positions (zones) along the inspiratory path. Such zonation would enable a dynamic behavioral strategy for maximizing the efficacy of sorptiveness as a relevant odorant feature [35,66]. That is, animals could regulate their sampling behavior dynamically, to match incoming stimulus representations to existing odor memories, to emphasize either discriminability or generalization, or to assess the features of similarity among stimuli. Additionally, animals could adjust their sniffing to direct particular odotopes to the most responsive ORNs, particularly when such ORNs are positioned in areas not well matched for the intrinsic sorptiveness of the odorant [12,35]. This flexibility could also contribute to perceptual resiliency following substantial damage to the OE or MOB [67].

Finally, and most significantly, odor sampling could be more similar to other sensory sampling behaviors such as visual saccades and somatosensory investigation than is currently appreciated. That is, odor identification might not normally be performed using single samples, particularly in the context of complex natural scenes. Rather, repeated or extended sniffs with varying sampling parameters might be used to construct an identifiable odor image by integrating information gained over multiple sequential samples, possibly affording access to subtleties in the odor signature that could not be appreciated with only a single sniff. This view is certainly consonant with behavioral findings, including the observation that more difficult discriminations require longer temporal integration of olfactory sampling than do simple discriminations [68]. It also emphasizes the importance of understanding the influence of odor memory, behavioral context and olfactory cortical–bulbar networks on the sampling, representation and processing of olfactory stimuli [69].

Evaluation of the zonation hypothesis will require concerted efforts to manipulate and/or measure sniffing behavior, as well as the sorptive properties of test odorants, in olfactory physiological and behavioral studies. Will freely behaving animals significantly adjust their sniffing when confronted with odorants differing substantially in sorptiveness, as they do in response to odorants of differing concentrations [36]? Will manipulation of airflow rates or other artificial sniffing parameters in anesthetized animals significantly affect odorant-induced activity in the MOB as it does in the OE [63]? These and similar questions deserve further attention.

Concluding remarks

The apparent anatomical adaptations of the rodent nose reviewed here are likely to enhance the efficacy of olfactory zonation and sampling, consistent with the central importance of olfaction in these species. Rodent nasal anatomy facilitates laminar airflow and hence is likely to augment nasal chromatography along discrete air passages. Spatially segregated zones of OR expression along these air passages enable this chromatographic separation to be translated into differential patterns of OR activation, which in turn can be regulated by the motor dynamics of sampling behavior (sniffing). This promotes greater discriminability among odorants, while in principle enabling recognition of the similarities between odotopes on molecules of very different sorptive properties. Challenges for future work will be to test whether rodents actually use these additional faculties that they appear to possess, and to identify under what circumstances such use contributes to perception.

Acknowledgements

We thank Tom Bozza for early discussions on many of the points raised in this review. Our own work, as cited here, has been generously supported by the National Institutes of Health. The views expressed in this paper are entirely our own.

References

1 Buck, L. and Axel, R. (1991) A novel multigene family may encode odorant receptors: a molecular basis for odor recognition. *Cell* 65, 175–187
2 Axel, R. (1995) The molecular logic of smell. *Sci. Am.* 273, 154–159
3 Feinstein, P. and Mombaerts, P. (2004) A contextual model for axonal sorting into glomeruli in the mouse olfactory system. *Cell* 117, 817–831
4 Gao, Q. *et al*. (2000) Convergent projections of *Drosophila* olfactory neurons to specific glomeruli in the antennal lobe. *Nat. Neurosci.* 3, 780–785
5 Dynes, J.L. and Ngai, J. (1998) Pathfinding of olfactory neuron axons to stereotyped glomerular targets revealed by dynamic imaging in living zebrafish embryos. *Neuron* 20, 1081–1091
6 Mombaerts, P. *et al*. (1996) Visualizing an olfactory sensory map. *Cell* 87, 675–686
7 Araneda, R.C. *et al*. (2000) The molecular receptive range of an odorant receptor. *Nat. Neurosci.* 3, 1248–1255
8 Igarashi, K.M. and Mori, K. (2005) Spatial representation of hydrocarbon odorants in the ventrolateral zones of the rat olfactory bulb. *J. Neurophysiol.* 93, 1007–1019
9 Bozza, T. *et al*. (2002) Odorant receptor expression defines functional units in the mouse olfactory system. *J. Neurosci.* 22, 3033–3043
10 Lodovichi, C. *et al*. (2003) Functional topography of connections linking mirror-symmetric maps in the mouse olfactory bulb. *Neuron* 38, 265–276
11 Feinstein, P. *et al*. (2004) Axon guidance of mouse olfactory sensory neurons by odorant receptors and the β2 adrenergic receptor. *Cell* 117, 833–846
12 Johnson, B.A. *et al*. (2005) Interactions between odorant functional group and hydrocarbon structure influence activity in glomerular response modules in the rat olfactory bulb. *J. Comp. Neurol.* 483, 205–216
13 Illig, K.R. and Haberly, L.B. (2003) Odor-evoked activity is spatially distributed in piriform cortex. *J. Comp. Neurol.* 457, 361–373
14 Malnic, B. *et al*. (1999) Combinatorial receptor codes for odors. *Cell* 96, 713–723
15 Zou, Z. *et al*. (2001) Genetic tracing reveals a stereotyped sensory map in the olfactory cortex. *Nature* 414, 173–179
16 Cutforth, T. *et al*. (2003) Axonal ephrin-As and odorant receptors: coordinate determination of the olfactory sensory map. *Cell* 114, 311–322
17 Rubin, B.D. and Katz, L.C. (2001) Spatial coding of enantiomers in the rat olfactory bulb. *Nat. Neurosci.* 4, 355–356
18 Xu, F. *et al*. (2000) Odor maps in the olfactory bulb. *J. Comp. Neurol.* 422, 489–495
19 Wallace, D.G. *et al*. (2002) Rats can track odors, other rats, and themselves: implications for the study of spatial behavior. *Behav. Brain Res.* 131, 185–192

20 Marchand, J.E. *et al*. (2004) Olfactory receptor gene expression in tiger salamander olfactory epithelium. *J. Comp. Neurol.* 474, 453–467
21 Strotmann, J. *et al*. (2004) Olfactory receptor proteins in axonal processes of chemosensory neurons. *J. Neurosci.* 24, 7754–7761
22 Kimbell, J.S. *et al*. (1997) Computer simulation of inspiratory airflow in all regions of the F344 rat nasal passages. *Toxicol. Appl. Pharmacol.* 145, 388–398
23 Zhao, K. *et al.* Numerical modeling of airway odorant transport during sniffing in the human and rat nose. *Chem. Senses* (in press)
24 Zhao, K. *et al*. (2004) Effect of anatomy on human nasal air flow and odorant transport patterns: implications for olfaction. *Chem. Senses* 29, 365–379
25 Goldman, J.A. and Koehl, M.A.R. (2001) Fluid dynamic design of lobster olfactory organs: high speed kinematic analysis of antennule flicking by *Panulirus argus*. *Chem. Senses* 26, 385–398
26 Keyhani, K. *et al*. (1997) A numerical model of nasal odorant transport for the analysis of human olfaction. *J. Theor. Biol.* 186, 279–301
27 Mozell, M.M. and Jagodowicz, M. (1973) Chromatographic separation of odorants by the nose: retention times measured across *in vivo* olfactory mucosa. *Science* 181, 1247–1249
28 Medinsky, M.A. *et al*. (1993) Advances in biologically based models for respiratory tract uptake of inhaled volatiles. *Fundam. Appl. Toxicol.* 20, 265–272
29 Morris, J.B. *et al*. (1986) Species differences in upper respiratory tract deposition of acetone and ethanol vapors. *Fundam. Appl. Toxicol.* 7, 671–680
30 Kurtz, D.B. *et al*. (2004) Experimental and numerical determination of odorant solubility in nasal and olfactory mucosa. *Chem. Senses* 29, 763–773
31 Jennings, W. *et al*. (1997) *Analytical Gas Chromatography*, Academic Press
32 Mozell, M.M. *et al*. (1991) The effect of flow rate upon the magnitude of the olfactory response differs for different odorants. *Chem. Senses* 16, 631–649
33 Kent, P.F. *et al*. (1996) The interaction of imposed and inherent olfactory mucosal activity patterns and their composite representation in a mammalian species using voltage-sensitive dyes. *J. Neurosci.* 16, 345–353
34 Sobel, N. *et al*. (1999) The world smells different to each nostril. *Nature* 402, 35
35 Youngentob, S.L. *et al*. (1987) A quantitative analysis of sniffing strategies in rats performing odor detection tasks. *Physiol. Behav.* 41, 59–69
36 Sobel, N. *et al*. (2000) Sniffing longer rather than stronger to maintain olfactory detection threshold. *Chem. Senses* 25, 1–8
37 Schoenfeld, T.A. *et al*. (1994) The spatial organization of the peripheral olfactory system of the hamster. Part I: receptor neuron projections to the main olfactory bulb. *Brain Res. Bull.* 34, 183–210
38 Clancy, A.N. *et al*. (1994) The spatial organization of the peripheral olfactory system of the hamster. Part II: receptor surfaces and odorant passageways within the nasal cavity. *Brain Res. Bull.* 34, 211–241
39 Schoenfeld, T.A. and Knott, T.K. (2002) NADPH diaphorase activity in olfactory receptor neurons and their axons conforms to a rhinotopically-distinct dorsal zone of the nasal cavity and main olfactory bulb. *J. Chem. Neuroanat.* 24, 269–285
40 Schoenfeld, T.A. and Knott, T.K. (2004) Evidence for the disproportionate mapping of olfactory airspace onto the main olfactory bulb of the hamster. *J. Comp. Neurol.* 476, 186–201
41 Christensen, T.A. and White, J. (2000) Representation of olfactory information in the brain. In *The Neurobiology of Taste and Smell* (2nd edn) (Finger, T.E. *et al*., eds), pp. 201–232, John Wiley & Sons
42 Iwema, C.L. *et al*. (2004) Odorant receptor expression patterns are restored in lesion-recovered rat olfactory epithelium. *J. Neurosci.* 24, 356–369
43 Miyamichi, K. *et al*. (2005) Continuous and overlapping expression domains of odorant receptor genes in the olfactory epithelium determine the dorsal/ventral positioning of glomeruli in the olfactory bulb. *J. Neurosci.* 25, 3586–3592
44 Levai, O. *et al*. (2003) Subzonal organization of olfactory sensory neurons projecting to distinct glomeruli within the mouse olfactory bulb. *J. Comp. Neurol.* 458, 209–220
45 Strotmann, J. *et al*. (2000) Local permutations in the glomerular array of the mouse olfactory bulb. *J. Neurosci.* 20, 6927–6938
46 Pyrski, M. *et al*. (2001) The OMP-lacZ transgene mimics the unusual expression pattern of OR-Z6, a new odorant receptor gene on mouse chromosome 6: implication for locus-dependent gene expression. *J. Neurosci.* 21, 4637–4648
47 Schwarting, G.A. *et al*. (2004) Semaphorin 3A-mediated axon guidance regulates convergence and targeting of P2 odorant receptor axons. *Eur. J. Neurosci.* 19, 1800–1810
48 Taniguchi, M. *et al*. (2003) Distorted odor maps in the olfactory bulb of semaphorin 3A-deficient mice. *J. Neurosci.* 23, 1390–1397
49 Hamlin, J.A. *et al*. (2004) Differential expression of the mammalian homologue of fasciclin II during olfactory development *in vivo* and *in vitro*. *J. Comp. Neurol.* 474, 438–452
50 Alenius, M. and Bohm, S. (2003) Differential function of RNCAM isoforms in precise target selection of olfactory sensory neurons. *Development* 130, 917–927
51 Aungst, J.L. *et al*. (2003) Centre-surround inhibition among olfactory bulb glomeruli. *Nature* 426, 623–629
52 Hayar, A. *et al*. (2004) External tufted cells: a major excitatory element that coordinates glomerular activity. *J. Neurosci.* 24, 6676–6685
53 Luo, M. and Katz, L.C. (2001) Response correlation maps of neurons in the mammalian olfactory bulb. *Neuron* 32, 1165–1179
54 Schoenfeld, T.A. *et al*. (1985) Topographic organization of tufted cell axonal projections in the hamster main olfactory bulb: an intrabulbar associational system. *J. Comp. Neurol.* 235, 503–518
55 Liu, W-L. and Shipley, M.T. (1994) Intrabulbar associational system in the rat olfactory bulb comprises cholecystokinin-containing tufted cells that synapse onto the dendrites of GABAergic granule cells. *J. Comp. Neurol.* 346, 541–558
56 Schoenfeld, T.A. and Macrides, F. (1984) Topographic organization of connections between the main olfactory bulb and pars externa of the anterior olfactory nucleus in the hamster. *J. Comp. Neurol.* 227, 121–135
57 Zhang, X. *et al*. (2004) High-throughput microarray detection of olfactory receptor gene expression in the mouse. *Proc. Natl. Acad. Sci. U. S. A.* 101, 14168–14173
58 Cleland, T.A. and Linster, C. (1999) Concentration tuning mediated by spare receptor capacity in olfactory sensory neurons: a theoretical study. *Neural Comput.* 11, 1673–1690
59 Hudspeth, A.J. (2000) Sensory transduction in the ear. In *Principles of Neural Science* (4th edn) (Kandel, E.R. *et al*., eds), pp. 614–624, McGraw-Hill
60 Zhang, X. and Firestein, S. (2002) The olfactory receptor gene superfamily of the mouse. *Nat. Neurosci.* 5, 124–133
61 Scott, J.W. *et al*. (2000) Chemical determinants of the rat electro-olfactogram. *J. Neurosci.* 20, 4721–4731
62 Norlin, E.M. *et al*. (2005) Odorant-dependent, spatially restricted induction of c-fos in the olfactory epithelium of the mouse. *J. Neurochem.* 93, 1594–1602
63 Scott-Johnson, P.E. *et al*. (2000) Effects of air flow on rat electro-olfactogram. *Chem. Senses* 25, 761–768
64 Vedin, V. *et al*. (2004) Zonal ablation of the olfactory sensory neuroepithelium of the mouse: effects on odorant detection. *Eur. J. Neurosci.* 20, 1858–1864
65 Scott, J.W. Sniffing and spatiotemporal coding in olfaction. *Chem. Senses* (in press)
66 Cleland, T.A. *et al*. (2002) Behavioral models of odor similarity. *Behav. Neurosci.* 116, 222–231
67 Slotnick, B. and Bodyak, N. (2002) Odor discrimination and odor quality perception in rats with disruption of connections between the olfactory epithelium and olfactory bulbs. *J. Neurosci.* 22, 4205–4216
68 Abraham, N.M. *et al*. (2004) Maintaining accuracy at the expense of speed: stimulus similarity defines odor discrimination time in mice. *Neuron* 44, 865–876
69 Wilson, D.A. and Stevenson, R.J. (2003) The fundamental role of memory in olfactory perception. *Trends Neurosci.* 26, 243–247